

# Acquisition of Weak GNSS Signals Using a New Block Averaging Pre-Processing

Mohamed Sahmoudi<sup>1</sup>, René Jr. Landry<sup>1</sup> and Moeness G. Amin<sup>2</sup>

<sup>1</sup> Navigation Research Groupe (NRG), LACIME Lab.

Ecole de Technologie Supérieure (ETS)

Montréal, Québec, Canada

<sup>2</sup>Wireless Communications and Positioning Lab

Center for Advanced Communications

Villanova University, Villanova, PA 19085, USA

**Abstract**—In this paper, we introduce a new approach for the acquisition of weak GNSS signals. For the GPS L1 signal, we utilize the replication property of the C/A code within each data bit to introduce a block averaging pre-processing (BAP) approach for improving receiver robustness against undesired signals. A large number of weighted signal blocks is accumulated and synchronously averaged to obtain a single block with improved signal power. We present several properties of the proposed GNSS signals enhancement technique and we analyze its robustness against noise and different classes of interferers. Thus, we develop a software defined acquisition procedure using the efficient FFT correlation approach. We propose two acquisition algorithms based on the BAP approach. The first scheme implements the parallel code phase search in finding the 2-D spectrum peak using circular cross-correlations. In the second scheme, we exploit the BAP for a fast acquisition performing the frequency estimation prior to the 1-D code-phase search.

## I. INTRODUCTION

Global Navigation Satellite Systems (GNSS), such as the US GPS and the European Galileo, are based on the principle that user's position can be determined from distances measured to objects with known positions [10]. From the propagation time measurements to at least four satellites, the user's coordinates in three-dimensional space can be determined, in addition to an estimate of the clock offset between the user and system clocks [10], [15, ch. 2], [20, ch. 2]. Despite the ever increasing civilian applications, significant limitations of the current GPS arise from interference and, more importantly, multipath propagation as well as insufficient signal strength when operating in city canyons and indoor [9], [20, ch. 14-15], [27], [28]. The effect of interference is to reduce the signal-to-noise ratio (SNR) of the GNSS signal such that the GNSS receiver is unable to obtain measurements from the GNSS satellite [15, ch. 6], [20, ch. 20], [27]. The direct-sequence spread-spectrum (DS-SS) scheme, which underlines the GNSS signal structure, provides a certain degree of protection against interference. However, when the jammer power is much stronger than the signal power, the spreading gain alone is insufficient to yield any meaningful information [20, ch. 20], [27]. Interference is typically mitigated prior to the correlation loops using temporal, special and spectral distinctions between the GNSS and undesired signals [3], [4], [26].

Conventional GPS receivers process blocks of one millisecond of signal coherently and extend the integration time non-coherently [15, ch. 5], [27]. For weak signals, receiver sensitivity can be amplified if longer durations of signal are processed coherently [2], [8], [25], [27]. However, without external aiding, the existence of navigation bit transition limits the coherent integration period to 20 ms. For indoor GNSS applications, the data stream may be provided from cellular networks [8], [9]. The binary data can be then used in a feedback scheme for self-aiding to extend the coherent integration time of the tracking loop [30]. In the case when external assistance is not available, the navigation data can be estimated while the synchronization process is on-going [30].

This paper deals with signal acquisition, specifically for low SNR environments. We improve the GNSS acquisition robustness against weak signal effects and undesired signals. We consider a data segment of 20 ms length and use a successive sign reversal of 1 ms signal block for data bit transition detection and correction. In essence, we operate on the data-bit edge free version of the received signal. The sign reversal technique was discussed in [29] and is applied here in the despreading process to utilize the entire twenty blocks free from data bit transition in the acquisition phase.

A block averaging pre-processing (BAP) scheme is introduced involving long coherent integration to increase the GNSS signal strength by a factor equal to the number of used code blocks. We apply the Fast Fourier Transform (FFT)-based parallel code phase search algorithm [5] to the weighted average of the data code blocks, rather than considering only one or extended data block, as has commonly been the case. The weights are responsible for the in-phase alignment of the code blocks. Finding the phase change for in-phase blocks accumulation is achieved by searching the carrier frequency offset over the narrow frequency range [0, 1 KHz]. The code phase and Doppler frequency are then estimated by cross-correlation using frequency domain data manipulations. The paper also proposes fast implementation that is suitable for moderate to high SNR signal acquisition.

## II. GPS SIGNAL MODEL

Consideration of multipath in a GNSS is typically in the context of signal code and carrier tracking accuracies, since these receiver functions are more sensitive to multipath degradation than signal acquisition or data modulation [15]. In this paper, we exclude multipath signals when considering signal acquisition analysis and processing. In addition, we focus our analysis on the current operating GPS system with the L1 C/A code signals. Thus, the input receiver signal from a given satellite can be expressed in the complex form as,

$$r(t) = Ad(t)c(t)e^{j[2\pi(f_c+f_d)t+\varphi_0]} + J(t) + w(t) \stackrel{\text{def}}{=} s(t) + v(t) \quad (1)$$

where  $A$  is the GPS signal amplitude,  $d(t)$  is the navigation data,  $f_c = 1575.42$  MHz is the L1 carrier frequency,  $f_d$  is the frequency offset due to Doppler, which is typically within the range of  $f_d \in [-10 \text{ KHz}, +10 \text{ KHz}]$  [27], and  $\varphi_0$  is the phase offset. The spreading waveform of the current GPS L1 signal is a binary phase-shift keying (BPSK) signal,

$$c(t) = \sum_{n=0}^{P-1} c(n)g(t - nT_c), \quad (2)$$

obtained by convolving the pseudo-random noise (PRN) impulse sequence of length  $P = T/T_c$  with a rectangular chip-shaping pulse  $g(t)$ , where  $T_c$  is the pulse duration and  $T$  is the integration time in the GPS receiver. The C/A code has a chip rate of  $1/T_c = 1.023$  MHz, so a chip is of period  $T_c = 977.5$  ns ( $1023 \times 10^3$  chips/second). One period of the spreading C/A code consists of 1023 chips, hence it spans 1 millisecond, and there are twenty 1 ms code epochs (blocks) in each GPS BPSK data bit. In the above equation,  $s(t)$  denotes the signal portion of the received data. The interference plus Gaussian noise term is denoted by  $v(t) \stackrel{\text{def}}{=} J(t) + w(t)$ .

Based on the GPS front-end configuration, the received GPS signal is downconverted and sampled using a sampling frequency  $f_s$ . We assume  $f_s$  to be an integer multiple of 1 KHz so that the number of data samples in each block is an integer. With knowledge of the GPS L1 carrier frequency, the received signal can be translated to baseband and, as such, the sampled data model can be expressed as,

$$r(n) = Ad(nT_s)c(nT_s)e^{j(2\pi f_d nT_s + \varphi_0)} + v(nT_s) = s(n) + v(n), \quad (3)$$

where  $T_s = 1/f_s$  is the sample period.

Pre-correlation noise and interference mitigation is an important function in GPS acquisition [15]. This task is generally aided by extending the coherent integration interval, providing that data bit transitions and the increase in Doppler frequency resolution are tolerated [27].

## III. BLOCK AVERAGING PRE-PROCESSING OF WEAK GPS SIGNALS

Recently, the application of block processing techniques to GNSS signals has received widespread interest due to their potential in improving the performance and capabilities of navigation receivers [11], [13], [21]. A block processor operates on blocks of data rather than processing the data samples sequentially. The block size is usually chosen to be

an integer multiple of the length of the spreading code. For GPS C/A code processing, the minimum block size is the length of the C/A code, which spans 1023 chips of duration 1 ms. The GPS receiver uses typically one spreading code; i.e. one block for coherent integration during acquisition. However, weak GPS signals require longer data sequences. Existing approaches, typically process blocks of the cross-correlation outputs between the received signal and local code [11], [13], [21]. In this paper, a different approach is proposed which calls for pre-processing (weighting, accumulating and averaging) blocks of the received signal prior to despreading. This requires the compensation of the phase change across several consecutive data blocks. The proposed pre-processing enables pre-correlation noise plus interference power reduction and allows fast receiver startup.

Consider  $N$  samples of  $r(n)$  for each 1 ms data block and accumulate signal samples over  $L$  ms, where  $L$  is an integer such that  $L \in \{1, \dots, 20\}$ . Accordingly, the total number of data samples considered is  $NL$ . Exploiting the replication property of the C/A code, and since  $NT_s = 1$  ms, we can write  $c(nT_s) = c((n+iN)T_s)$  for any integer  $i$ . As we mentioned earlier, accumulating multiple blocks of the GPS signal for a coherent integration faces outstanding problems, especially the data bit edge problem. There is two widely used techniques to deal with a possible data bit transition within a 20 ms coherent integration. The first approach consists of running two consecutive 10 ms coherently integrated sums. Then, the first 10 ms or the second 10 ms is guaranteed to be free of data bit transition [27]. The second method consists of maintaining twenty running sums, each delayed by 1 ms relative to its predecessor [21]. These running sums actually extend over two data bit intervals. If there is a transition, the sum that aligns with the transition produces the maximum value. This technique is useful when the residual frequency error is small. In [29], a new technique called BACIX is proposed, wherein twenty running sums are maintained but each sum successively reverses the sign of one sample of the previous sum. The matched reversal rectifies all samples to the same sign, thus producing the maximum value for the sum. In contrast to the previous technique [21], this method allows sign correction using only one data bit, i.e, 20 ms. Thus, using the sign correction technique [29], the data bit is considered constant over  $L$  data blocks, and we can write  $d(nT_s) = d((n+iN)T_s)$  for any integer  $i$ . Accordingly, by averaging the input data over  $L$  consecutive blocks, as illustrated by the diagram given in Figure 1, we obtain the averaged data block,

$$\begin{aligned} r_L(n) &\stackrel{\text{def}}{=} \frac{1}{L} \sum_{i=0}^{L-1} r(n+iN) \\ &= Ad(nT_s)c(nT_s)e^{j[2\pi f_d nT_s + \varphi_0]} H_L(f_d) + v_L(n) \\ &= H_L(f_d)s(n) + v_L(n) \end{aligned} \quad (4)$$

where  $H_L(f_d) = \frac{1}{L} \sum_{i=0}^{L-1} e^{j2\pi f_d iNT_s}$  represents the block average signal coefficient or the BAP response and  $v_L(n) = \frac{1}{L} \sum_{i=0}^{L-1} v(n+iN)$  is the block average of the undesired signal component.

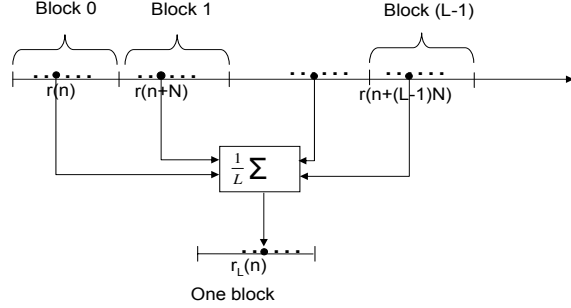


Fig. 1. Block-averaging for long coherent integration over  $L$  data blocks of 1ms of the received weak GPS signal.

The BAP response  $H_L(f_d)$  can be expressed as,

$$\begin{aligned} H_L(f_d) &= \frac{1}{L} \sum_{i=0}^{L-1} e^{j2\pi f_d i N T_s} \\ &= \frac{1}{L} \left[ \frac{\sin(\pi f_d N T_s L)}{\sin(\pi f_d N T_s)} \right] e^{j\pi f_d N T_s (L-1)}. \end{aligned} \quad (5)$$

In that case, Figure 1 depicts the proposed block-averaging signal pre-processing (BAP) scheme, which is equivalent to applying a finite impulse response (FIR) filter with impulse response,

$$h_L(n) = \frac{1}{L} \sum_{i=0}^{L-1} \delta(n + iN) = \begin{cases} \frac{1}{L} & \text{for } 0 \leq \frac{n}{N} \leq L-1, \\ 0, & \text{otherwise.} \end{cases} \quad (6)$$

where  $\delta(\cdot)$  is a unit sample function. According to equation (6), the BAP filter acts as a frequency selective lowpass filter, because of its effect as a truncation function similarly to the rectangular function. That is, the BAP filter applies a decimated version of the window, i.e.  $h_L(n) = (1/L)w_r(n)$ , where  $w_r(n)$  is the rectangular window of length  $L$  [19]. The above function assumes peak values at frequencies which are a multiple integer of 1 KHz. The zero-crossing bandwidth is  $2/L$  KHz. Accordingly, it can be concluded that if the GPS signal whose Doppler frequency is within the range of  $[k \pm 2/L]$  KHz, where  $k$  is an integer number, then the signal lies in the filter mainlobe and will benefit from the BAP scheme. Jammer signals, whether they are narrowband or broadband, outside the above frequency band will encounter power reduction. Further, the noise variance will be reduced by a factor of  $L$ , as a result of BAP. The goal of block-averaging is now clear. We need to perform an appropriate weighted sum of the successive code blocks such that the result is within the mainlobe of the employed window. Figure 2 depicts the amplitude response function  $|H_L(f_d)|$  for different block number  $L$ . It is evident that larger values of  $L$  lead to finer

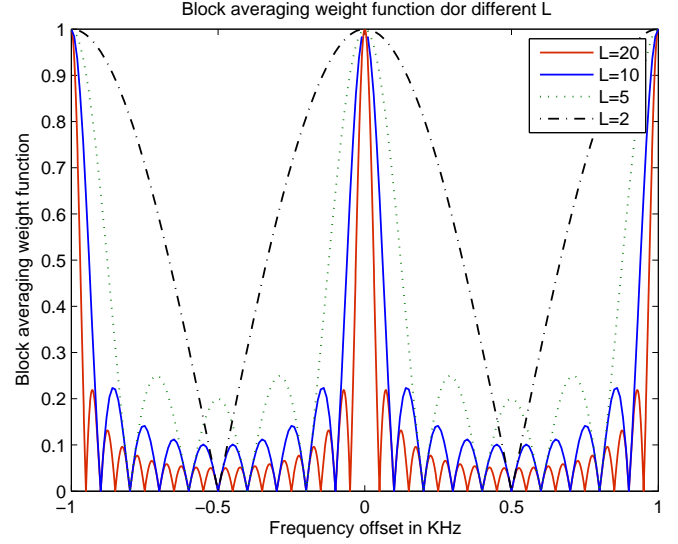


Fig. 2. Block-averaging gain function versus frequency offset for different block number  $L$ .

resolution. Since the frequency  $f_d$  is unknown, the maximum of this weight may not be achieved. Therefore, our aim is to keep the same GPS signal strength by achieving the maximum value of the weight function  $H_L(f_d)$  while reducing the noise and interference power after accumulating and averaging the  $L$  data blocks. This provide more opportunity to mitigate sidelobe jammers, but puts more demands on the accuracy of the in-phase alignment of the GPS code blocks. With fixed  $L$ , the use of different windows in place  $w_r(n)$  may change the nature of the tradeoff between mainlobe width and sidelobe heights, however, it does not remove it [19].

In other words, the BAP processing is a sum operation of sinusoidal signals with the same frequency that results in a similar signal with a different phase offset. This is an additional phase drift due to the extended coherent integration. In order to obtain in-phase alignment, or to force the block averaging to lie within the employed window mainlobe, we need to estimate the unknown frequency offset  $f_d$  from the  $k$  KHz and compensate for it prior to averaging. To proceed, we define a special block-averaging for phase compensation, while assuming constant Doppler variation over the integration time, which is a valid assumption for most civil applications [27]. In essence, in the rest of this paper we suggest to multiply the baseband signal with weights represented by the frequency component  $\beta(n) = e^{j2\pi\delta f n T_s}$ ,

$$\begin{aligned} \tilde{r}(n) &= r(n)e^{j2\pi\delta f n T_s} \\ &= A d(n T_s) c(n T_s) e^{j[2\pi\tilde{f} n T_s + \tilde{\varphi}_0]} + v(n T_s) e^{j2\pi\delta f n T_s} \\ &\stackrel{\text{def}}{=} \tilde{s}(n) + \tilde{v}(n) \end{aligned} \quad (7)$$

where  $\tilde{f} = f_d + \delta f$  and  $\tilde{\varphi}_0$  combines the initial phase  $\varphi_0$  and the constant phase difference between the local carrier and the incoming signal. The component  $\tilde{s}(n)$  denotes the signal portion of the new data sequence and  $\tilde{v}(n)$  is the noise plus interference term after phase correction. It is important to note that the intent is to estimate  $\delta f$  such that  $\tilde{f}$  is not

necessary zero, but rather an integer multiple of 1 KHz, so  $H_L(f_d + \delta f) = 1$ . This way, we benefit from block-averaging by placing the result into anyone of the mainlobes of the BAP response, as shown in Fig. 2. Accordingly,  $\delta f$  assumes values only in the range  $[0, 1]$  KHz. We use the fact that for any  $\tilde{f}$  integer multiple of 1 KHz,  $e^{j2\pi\tilde{f}iNT_s} = 1$  for each  $i \in \{0, \dots, L-1\}$ . The main difference between the sequence  $\tilde{r}(n)$  and  $r(n)$  is only the phase, while the C/A code information remains unchanged. To determine an optimal value of  $\delta f$ , a simple search is proposed in the next Section which deals with the acquisition process for the weak signal case. The proposed block averaging scheme is considered as an attractive coherent data compression technique for GPS signals pre-processing.

#### IV. ACQUISITION OF WEAK GPS SIGNAL USING BLOCK AVERAGING PRE-PROCESSING

##### A. Acquisition scheme

We apply the parallel code phase search acquisition algorithm [5], [27] to the frequency-compensated block averaged sequence  $\tilde{r}_L(n)$ . This FFT-based acquisition approach is a new trend in GNSS receivers for near instantaneous signal detection. It parallelizes the code space search dimension and uses circular correlation, i.e., instead of multiplying the input signal with a PRN code with 1023 different code phases, as performed in the serial search acquisition method, it makes a circular cross-correlation between the input and the PRN code without shifted code phase. In the following, we review the principle of circular correlation between two sequences  $x(n)$  and  $y(n)$  [5], [27]. Let  $X(k)$  and  $Y(k)$  denote the discrete Fourier transforms of  $x(n)$  and  $y(n)$ , with the same length  $N$ . Their circular cross-correlation  $z(n)$  of length  $N$  and periodic repetition is computed as

$$z(n) = \frac{1}{N} \sum_{m=0}^{N-1} x(m)y(m+n) = \frac{1}{N} \sum_{m=0}^{N-1} x(-m)y(m-n). \quad (8)$$

It is shown that the discrete  $N$ -point Fourier transform of  $z(n)$  can be expressed as  $Z(k) = X(k)^*Y(k)$ , where  $X(k)^*$  is the complex conjugate of  $X(k)$ . This relation provides a periodic (or circular) correlation. Once the frequency-domain representation of the cross-correlation is found, the time-domain representation can be found using inverse Fourier transform. More precisely, we develop an acquisition procedure by applying the recent parallel code phase search acquisition method to the output sequence of the BAP pre-processing. This procedure allows to process a compressed sequence of 1 ms length, and reduces the 2-D code phase-Doppler frequency search space to 1-D frequency search using the FFT-based circular cross-correlation [1], [27], [29], [30]. The Fourier transform of the local code must only be performed once during the acquisition stage.

To estimate  $\delta f$ , we consider a search over its range of 1 KHz. Furthermore, since an optimal value within  $[0, 500]$  Hz, implies another within  $[500, 1000]$  Hz, due to the symmetry around 500 Hz, we only search for  $\delta f$  in the range of  $[0, 500]$  Hz. We consider a 25 Hz as a reasonable frequency resolution

#### Parallel code phase search using the synchronously averaged data blocks

- Start the data bit detection: Consider a 20 ms data segment and process data bit detection with successive bit sign reversal [29]. Other technique also maybe used for this purpose.
  - ▶ PART 1: BLOCK AVERAGING PREPROCESSING BY DATA WEIGHTING
    - \* Step 1 - Multiplication with a local carrier: The incoming signal is multiplied by a locally generated carrier signal within a range of  $\frac{1}{2NT_s}$  Hz for BAP frequency compensation. We use a frequency step of 25 Hz and we generate 20 sequences in this step.
    - \* Step 2 - Block averaging: For each frequency value in Step 1, accumulate and average the twenty frequency compensated blocks.
  - ▶ PART 2: PARALLEL CODE PHASE SEARCH USING THE AVERAGE OF SYNCHRONIZED DATA BLOCKS
    - \* Step 3 - Multiplication with a local carrier within  $\pm 10$  KHz for Doppler frequency estimation: A frequency resolution of 500 Hz is a good choice compared to the typical value of 1 KHz.
    - \* Step 4 - Correlation in frequency domain using FFT and IFFT. Detect the 2-D correlation peak, then note the code phase value and the Doppler plus the optimal frequency compensation value. Finally, estimate the Doppler frequency  $f_d$  by subtracting the optimal value  $\delta f_0$ .
- End of data bit detection: Compare the twenty computed coherent sums. When a sufficiently strong peak is detected, then the acquisition is achieved and the receiver can begin tracking the estimated frequency and C/A code phase as needed to estimate the user position.

TABLE I

ACQUISITION ALGORITHM 1: BAP-BASED WEAK SIGNALS ACQUISITION

choice. Once the 2-D spectrum peak is detected at  $(f_d + \delta f_0)$ , we proceed to jointly estimate  $f_d$  and  $\delta f$ . Equivalently, the optimal frequency compensation  $\delta f_0$  is estimated by considering the block-averaging,

$$\begin{aligned} \tilde{r}_L(n) &= \frac{1}{L} \sum_{i=0}^{L-1} \tilde{r}(n + iN) \\ &= H_L(f + \delta f_0) \tilde{s}(n) + \tilde{v}_L(n) \quad (9) \\ &\approx \tilde{s}(n) + \tilde{v}_L(n), \quad (10) \end{aligned}$$

where  $\tilde{v}_L(n)$  is the reduced noise component after block-averaging of the phase-compensated data sequence. For the 2-D spectrum peak search, we apply the parallel code phase search acquisition method, as discussed in [1], [5], [27]. The overall proposed scheme is detailed in Table I. We search the code phase within one code and search the Doppler frequency  $f_d$  within a range of  $\pm 10$  KHz.

It should be mentioned that we only dealt with one satellite when expressing the received data, although there are more than one satellite in the field of view. Including multiple satellite signals in  $r(n)$  equation would only complicate the presentation without offering any tangible analytical or conceptual benefits. These additional satellites signals will be discriminated against in Step 4 of Table I through the local code cross-correlation process.

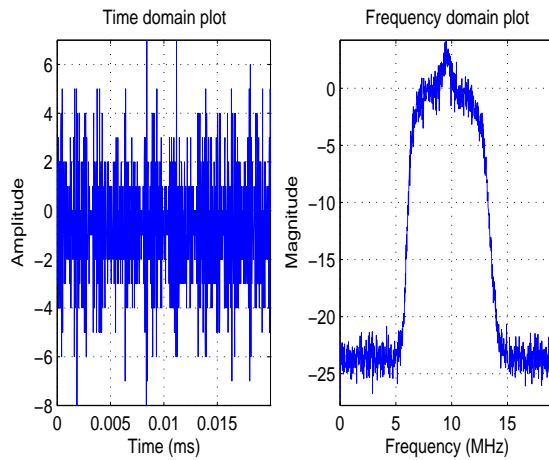


Fig. 3. Real GPS signal representation in time and frequency domains.

### B. Example of acquisition using real GPS satellites signals

We use a data set downloaded from the web site in [1]. These GPS signals were collected using a SIGE SE4110L front end GPS receiver. The parameters necessary for processing the data are as follows: Sampling Frequency of 38.192 MHz, Intermediate Frequency of 9.55 MHz (nominal), and the signed character is 8 bit sample format. In Fig. 3, the typical time - and frequency -domain representations of the employed data are illustrated. It is clear that the signal is similar to a Gaussian noise and no discernable structure is visible. In the frequency-domain, we notice the presence of the bandpass filter of 6 MHz bandwidth applied before sampling. Additionally, we see that in the center, there is a sinc function type behavior. This seems to be the mainlobe of the 2.046 MHz of the sinc spectrum of the GPS signal. Figure 4 shows the acquisition results using the parallel code phase search method. We observe that the four strong signals PRN 15, PRN 18, PRN 21 and PRN 22 were easily detected and acquired. However, as this method use only one block of data, it is unable to detect and acquire the other weak signals. In Figure 5, we show that using the proposed acquisition scheme over twenty data blocks, the additional weak signals PRN 3, PRN 6, PRN 9 and PRN 26 can be acquired. To further illustrate the comparative performance of the two methods, we show in Figure 6 that the correlation peaks are not clearly visible to be detected by the GPS receiver. However, these peaks are much more evident in Figure 7, in which a longer coherent integration time of 20 ms is implemented. As predicted by theoretical analysis, comparing Figure 6 and Figure 7, we observe the advantage of the BAP step in mitigating the zero-mean noise effect, that is, the extraneous false peaks are greatly reduced.

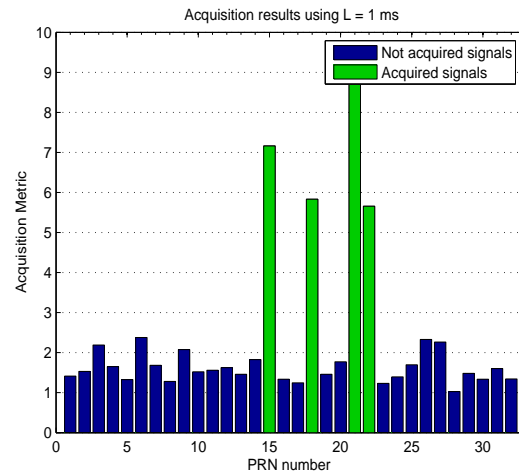


Fig. 4. Acquisition results using the parallel code phase search with integration over only one block:  $L = 1$  ms.

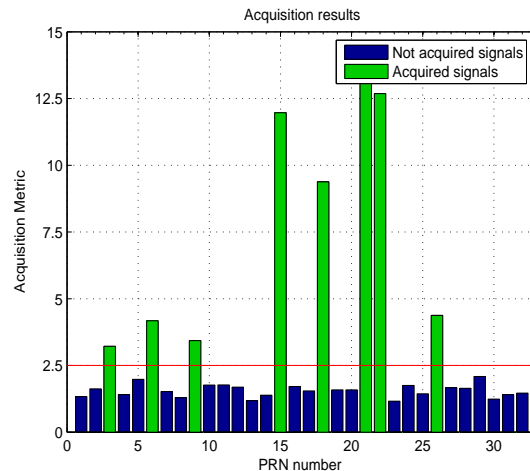
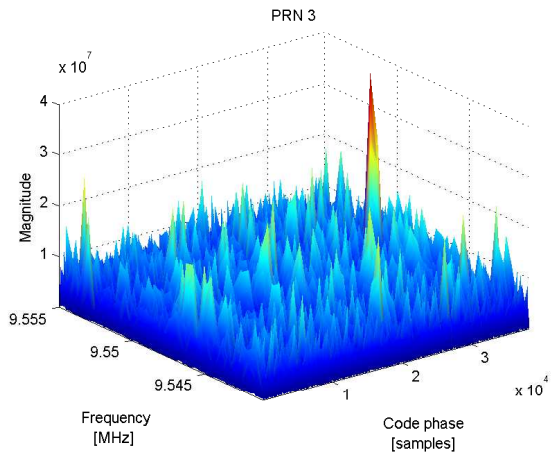
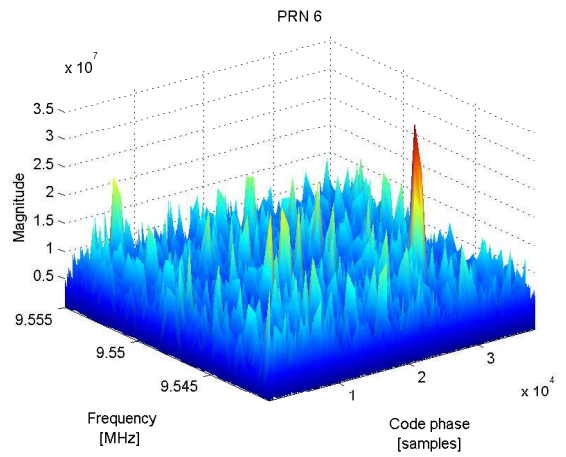


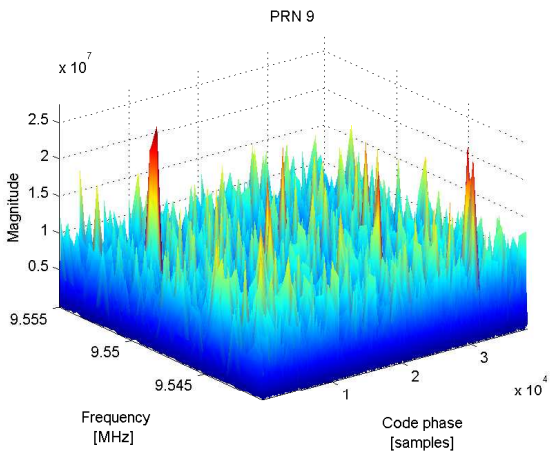
Fig. 5. Acquisition results using the proposed method for coherent integration of twenty blocks:  $L = 20$  ms.



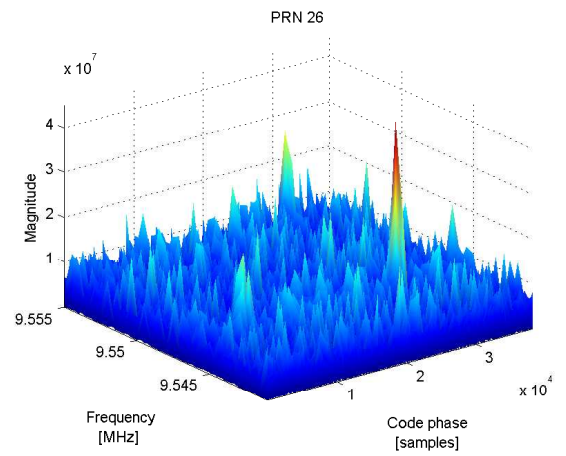
(a) Correlation output for the PRN number 3



(b) Correlation output for the PRN number 6

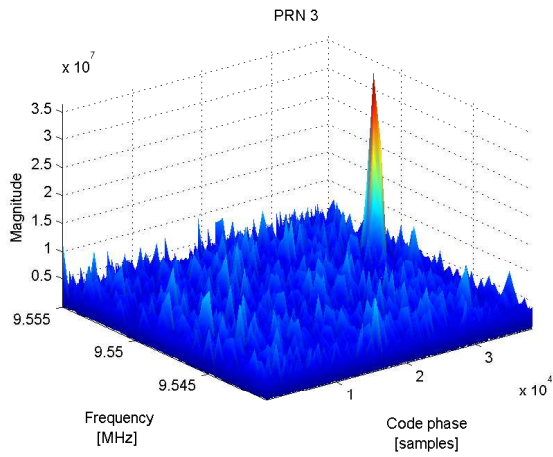


(c) Correlation output for the PRN number 9

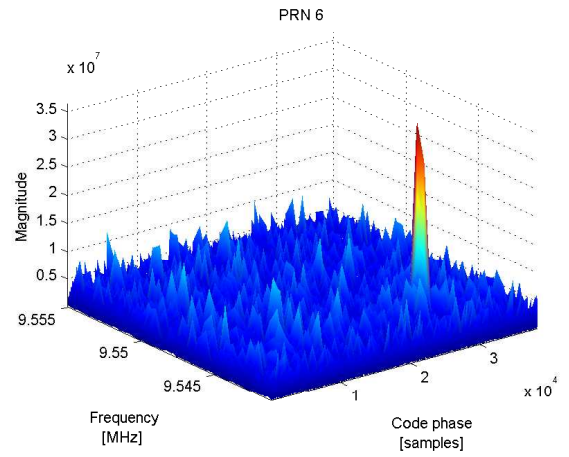


(d) Correlation output for the PRN number 26

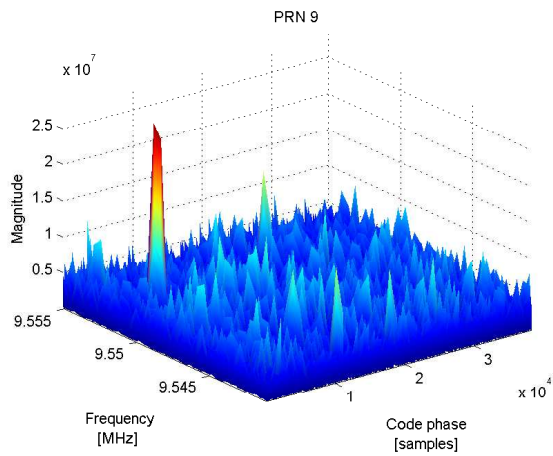
Fig. 6. Correlation output of the weak signals PRN 3, PRN 6, PRN 9 and PRN 26 using the parallel code search method over time integration of 1 ms.



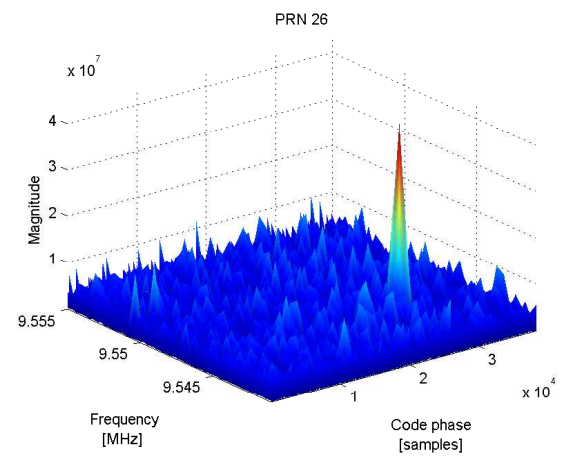
(a) Correlation output for the PRN number 3



(b) Correlation output for the PRN number 6



(c) Correlation output for the PRN number 9



(d) Correlation output for the PRN number 26

Fig. 7. Correlation output of the weak signals PRN 3, PRN 6, PRN 9 and PRN 26 using the proposed acquisition algorithm over time integration of 20 ms.

Step	BAP	circular correlation
Part 1: Weighting	$20LN$	
Part 2 : for each $\delta f_i$		
Step 3	$41N$	$41LN$
Step 4: Correlation		
Local code FFT		
Data FFT	$41N \log_2(N)$	$41LN \log_2(LN)$
Multiplication	$41N$	$41LN$
IFFT	$41N \log_2(N)$	$41LN \log_2(LN)$
Total	$20(L + 82)N$ $+1640N \log_2(N)$	$82LN(1 + \log_2(L))$ $+82LN \log_2(N)$
Total for $L = 20$	$2040N$ $+1640N \log_2(N)$	$\approx 8200N$ $+1640N \log_2(N)$
Total for $L = 40$	$2440N$ $+1640N \log_2(N)$	$\approx 19680N$ $+3280N \log_2(N)$

TABLE II

COMPLEXITY COMPARISON OF THE PROPOSED METHOD AND THE EXISTING ONE FOR EACH SIGNAL ACQUISITION.

### C. Computational load of the proposed acquisition scheme

In Table II, the computational complexity in Matlab flops is compared with that of the parallel code phase search acquisition algorithm, known also as circular cross-correlation method, using  $L$  blocks of data [2], [27]. The main advantage of the proposed acquisition approach, in comparison to the existing long coherent integration based methods, is that enhancing SNR is achieved without increasing the computational complexity.

In Table II, we do not count the FFT computations of the local code, since it can be done in advance and stored in the receiver. It is noted from Table II that the number of blocks  $L$  does not appear in the second part in the computational overhead of the proposed method, since we apply BAP prior to acquisition. According to the expressions in Table II, computations of the BAP-based method is equivalent to the existing method for  $L = 20$ . However, for  $L = 40$  the computation reduction is about 50 % compared to the standard approach. Thus, we conclude that the BAP-based scheme enhances the GPS signal power without changing the computational requirements for twenty blocks of data length. When using a higher number of data blocks, significant savings can be achieved.

## V. A FAST BAP-BASED ACQUISITION IMPLEMENTATION

### A. A BAP-based coherent / non-coherent integration

Based on the above BAP approach, we present below an alternative method for signal acquisition. It involves the spectrum estimation of the square value of the block-averaging sequence. We proceed with squaring the phase-compensated and averaged sequence, yielding,

$$\begin{aligned} \tilde{r}_L^2(n) &= e^{2j[2\pi\tilde{f}nT_s + \tilde{\varphi}_0]} + \tilde{v}_L^2(nT_s) \\ &+ \frac{2}{L} \tilde{v}_L(nT_s)d(nT_s)c(nT_s)e^{j[2\pi\tilde{f}nT_s + \tilde{\varphi}_0]}. \end{aligned} \quad (11)$$

We utilize the property  $d(nT_s)^2 = c(nT_s)^2 = 1$ . With a sufficient number of blocks, the FFT-based spectrum of  $\tilde{r}_L^2(n)$  will exhibit a strong dominant peak at the frequency  $2f$ .

The goal of the above squaring operation is to despread the C/A code enabling the estimation of the carrier frequency [27]. However, very noisy signals may render this approach unuseful, if applied without pre-processing. Accordingly, this procedure cannot be typically adopted for the original GPS signal. After BAP, the signal becomes sufficiently strong to detect the peak of the FFT-based spectrum of the squared sequence. With the estimate of  $(\delta f + f_d)$ , we can deduce the Doppler frequency  $f_d$ , as explained in Table III. Finally, we correlate with the local C/A codes to determine each PRN and code phase. In doing so, we only need to perform a one-dimensional search. All possible PRNs should be considered to determine each satellite and the code phase in the field of view.

Using the proposed block-averaging, the coherent gain of 10 ms is 10 dB and 13 dB for 20 ms, and additional gain must be obtained from non-coherent integrations. The main advantage is that we are combining coherent integration of 20 ms with non-coherent integrations using only this length of data. The novelty of this non-coherent implementation is that we are squaring and summing the outputs of coherent integrations of 20 ms. In addition, this is performed with computational cost equivalent to that used usually for 1 ms, because we compress the data using the BAP processing. Another issue is that in existing approaches, to combine 10 ms coherent integration with non-coherent integrations, we need to process multiples of this 10 ms.

### B. Computational load of the proposed coherent/non-coherent integration

The computational requirements of the acquisition method of Table III are as follows. Part 1 requires  $20LN$  flops, step 3 requires  $20N \log_2(N)$  flops, and step 4 requires  $2N \log_2(N)$  flops (for FFT and IFFT operations) for each satellite signal with a cost of  $8N \log_2(N)$ <sup>1</sup>. Step 5 requires repeating Step 4 for each of the 32 PRNs, so the number of flops during Step 4 and 5 is  $256N \log_2(N)$ . The total number of flops is, therefore,  $20LN + 256N \log_2(N)$ . Compared to Table III, the computational load has been significantly reduced and the fast implementation requires only about 11 % of the operations required by the conventional FFT-based circular cross-correlation acquisition.

Figure 8 illustrates the effectiveness of the squaring operation in conjunction with the block-averaging. It shows the spectrum magnitude of the square of the original signal (left) along with the spectrum magnitude of the square of the block-averaged sequence (right). We observe from Figure 8-(a) that FFT of  $r^2(n)$  has no clear peak while FFT of  $r_L^2(n)$  in Figure 8-(b) has a distinguished peak.

Figure 9-(a), depicts the FFT of the received signal correlated with the local code on the correct delay. After the BAP processing and correlation with the code at the correct delay, we depict the spectrum of the result in Figure 9-(b). A single clear peak is evident in this case, which demonstrates the

<sup>1</sup>We may stop the Doppler search in Steps 1-3 of Table III once four strong peaks are detected.

### Decoupled estimation of Doppler and code phase using BAP

- Start the data bit detection: Consider a 20 ms data segment and process data bit detection [29].
  - ▶ PART 1: BLOCK AVERAGING PREPROCESSING
    - \* Step 1 - Fine multiplication by a local carrier within 500 Hz: The incoming signal is multiplied by a locally generated carrier signal within a range of  $\frac{1}{2NT_s}$  Hz for BAP frequency compensation. We use a frequency step of 25 Hz, then we generate 20 sequences in this step.
    - \* Step 2 - Block averaging: For each frequency value of step 1, accumulate and average the twenty frequency compensated blocks together.
  - ▶ PART 2: DECOUPLED DOPPLER FREQUENCY AND CODE PHASE ESTIMATION
    - \* Step 3 - Square the block averaged data and detect its spectrum peak to estimate  $(f + \delta f)$ . Once the FFT peak is detected, obtain the Doppler frequency by subtracting the corresponding optimal  $\delta f$  value. To achieve the acquisition, we need in this step to find at least four strong peaks corresponding to four satellites.
    - \* Step 4 - Correlation with local codes: Since the Doppler has been estimated from step 3, the search becomes one-dimensional in the code phase.
    - \* Step 5 - Code phase identification: Repeat this procedure for all PRNs in the field of view.
- End of data bit detection.

TABLE III

ACQUISITION ALGORITHM 2: BAP-BASED FAST SIGNALS ACQUISITION ALGORITHM

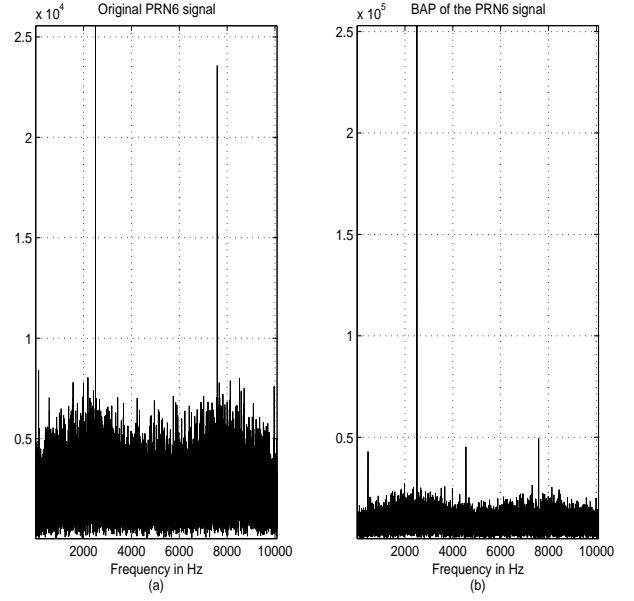


Fig. 9. Comparison of the FFT-based spectrum of a GPS signal and its block-averaged sequence. Digital frequency resolution is 500 Hz.

signal strength enhancement when using BAP prior to cross-correlation.

## VI. EFFECT OF THE BLOCK AVERAGING PRE-PROCESSING TO UNDESIRE SIGNALS

We show below that block averaging mitigates the noise and interference prior to the correlation processing. Three types of jammers are considered in addition to the Gaussian noise.

### A. Gaussian noise

If the GPS signal is corrupted by a zero-mean Gaussian noise  $w(t)$ , then the noise variance using  $L$  blocks becomes,

$$Var(w_L) = \frac{1}{L^2} \sum_{i=0}^L Var(w) = \frac{1}{L} Var(w). \quad (12)$$

That is, the BAP reduces the noise power by a factor of  $L$ , or equivalently increases the SNR by a factor of  $10\log_{10}(L)$  dB. For example, if we average a frequency-compensated sequence of an entire data bit period (i.e. 20 blocks), then we enhance the system SNR by 13 dB, which is definitely a welcomed gain for weak signal acquisition and processing. We note there are other ways to increase the GPS signal power using long coherent integration, but the proposed block averaging concept has two key advantages. First, unlike the accumulating block processing of [21] or the standard coherent integration in [27], the proposed method reduces the data input to one block (see Fig. 1), which is important for a rapide search of the C/A code and Doppler shift during the acquisition process. Second, the averaged short vector (1 ms interval) permits the use of a block average model for the maximum-likelihood delay estimation during the tracking and multipath mitigation process, as presented in [23].

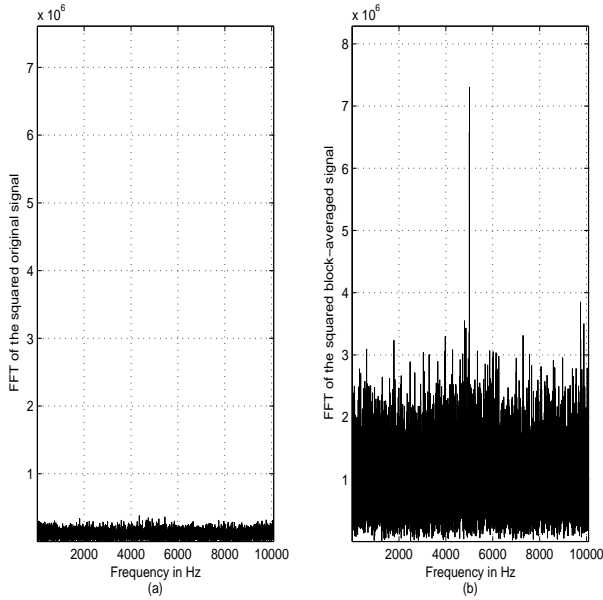


Fig. 8. Comparison of the FFT of a squared GPS signal and the FFT of its squared block-averaged sequence.

### B. Narrowband continuous wave (CW) jammer

CW is one of the most frequently encountered jamming signals, representing spectral lines in the frequency domain, and could appear at any time in the GPS spectrum. We express the CW interferer as  $J(nT_s) = J \cos(2\pi f_0 nT_s + \theta)$ , where  $J$  is the interference amplitude,  $f_0$  is the interference frequency offset relative to the GPS carrier, and  $\theta$  is its random uniform phase. The block averaging effect on the CW interference over  $L$  blocks is given by,

$$\begin{aligned} J_L(nT_s) &= \frac{1}{L} \sum_{i=0}^{L-1} J[(n+iN)T_s] \\ &= \frac{1}{L} \sum_{i=0}^{L-1} J \cos[2\pi f_0(n+iN)T_s + \theta] \end{aligned} \quad (13)$$

$$= \begin{cases} J(nT_s) & \text{if } f_0 = 0 \pmod{1\text{KHz}} \\ \frac{1}{L} \frac{\sin(\pi f_0 L)}{\sin(\pi f_0)} J [nT_s + \pi f_0(L-1)] & ; \text{ otherwise} \end{cases} \quad (14)$$

$$= \begin{cases} J(nT_s) & \text{if } f_0 = 0 \pmod{1\text{KHz}} \\ |H_L(f_0)| J [nT_s + \phi_L(f_0)] & ; \text{ otherwise.} \end{cases} \quad (14)$$

$$= J(nT_s) * h_L(n). \quad (15)$$

The following observations summarizes the impact of BAP on a CW interference:

- 1) If the frequency offset  $f_0$  of the CW jammer is within the frequency set  $\{k/L ; k \in \mathbb{Z}^*\}$  KHz, then BAP eliminates the jammer entirely.
- 2) If the frequency offset  $f_0$  of the CW jammer corresponds to the first sidelobe of amplitude, i.e.  $|H_L(f_0)| = S$ , then block averaging reduces the CW jammer power approximately by  $20 \log_{10}(L/S) = 13$  dB, and by more than 20 dB if  $f_0$  is within other sidelobes of  $|H_L(f_0)|$ .
- 3) In the presence of a CW jammer with frequency offset  $f_0 = 0 \pmod{1 \text{ KHz}}$ , the BAP has no effect on jammer mitigation. This of course represents the worst case scenario of a narrowband CW jamming, but it is likely improbable.

### C. Partial-band jammer

A partial-band jammer is an undesired signal that spreads its average power  $J_{av}$  evenly over some frequency range  $W_j$ , which is a subset of the GPS bandwidth  $W_s$ . We may express the jammer power as  $J_{av} = J_0 W_s$ , where  $J_0$  is the value of the power spectral density of an equivalent wideband jamming signal across the GPS band. This partial-band interference may be characterized by its power spectral density, given by

$$P_j(f) = \begin{cases} \frac{J_{av}}{W_j} = \frac{J_0 W_s}{W_j} & \text{if } |f| \leq \frac{1}{2} W_j \\ 0 & \text{if } |f| > \frac{1}{2} W_j, \end{cases} \quad (16)$$

where  $W_s \gg W_j$ . The mean square of the output of the BAP filter may be computed as,

$$\begin{aligned} \mathcal{E}_j^2 &= \int_{-\infty}^{+\infty} |H_L(f)|^2 P_j(f) df \\ &= \frac{J_{av}}{W_j} \int_{-W_j/2}^{+W_j/2} |H_L(f)|^2 df \\ &= \frac{J_{av}}{W_j L^2} \int_{-W_j/2}^{+W_j/2} \left| \frac{\sin(\pi f L)}{\sin(\pi f)} \right|^2 df. \end{aligned} \quad (17)$$

The above integral can be computed using Fourier series. The result is,

$$\mathcal{E}_j^2 = \frac{J_{av}}{L} \left[ 1 + \frac{1}{L} \frac{2}{\pi W_j} \sum_{k=1}^{L-1} (L-k) \frac{\sin(k\pi W_j)}{k} \right]. \quad (18)$$

After some straightforward calculations, we express the above equation into a closed form solution valid for large  $L$  as,

$$\mathcal{E}_j^2 = \frac{J_{av}}{L} \left[ \frac{1}{W_j} - \frac{2\Upsilon(L, W_j)}{L\pi W_j} \right], \quad (19)$$

where,

$\Upsilon(L, W_j) = [\cos(\frac{\pi W_j}{2}) - \cos((L-1/2)\frac{\pi W_j}{2})]/2 \sin(\frac{\pi W_j}{2})$ . From equations (18) and (19), we conclude that the block averaging is a useful tool for reducing the sub-band jammer power when using a large number of blocks  $L$ . In the limit as  $W_j$  becomes zero, the interference becomes an impulse at the carrier frequency. In this case, the interference is considered a CW, and the power spectral density is given as,  $P_{cw}(f) = J_{av} \delta(f_0)$ . The corresponding power is given by,

$$\mathcal{E}_{cw}^2 = J_{av} |H_L(f_0)|^2 = \frac{J_{av}}{L^2} \left| \frac{\sin(\pi f_0 L)}{\sin(\pi f_0)} \right|^2. \quad (20)$$

### D. In-band Chirp jammer

In addition to CW interference, a Chirp is one of the most commonly applied jammer signals. It is a wideband interference which is instantaneously narrowband. The spectrum of such a jammer may span all or part of the GPS frequency range. The Chirp jammer can be expressed as

$$J(t) = J e^{j\pi W t^2 / T}, \quad -T/2 \leq t \leq T/2. \quad (21)$$

Since the phase of  $J(t)$  varies quadratically over time, the frequency changes linearly versus  $t$ . Over the duration of the Chirp pulse, the jammer sweeps the frequencies from  $-W/2$  to  $+W/2$  Hz. In the frequency domain, the spectrum of the Chirp is concentrated in the range  $|f| < W/2$ . The parameters defining the Chirp jammer are the Chirp power level according to the interference to signal ratio (ISR) in dB, the Chirp pulse length  $T$ , referred to as the sweep duration (units generally in microseconds) and the Chirp swept bandwidth  $W$  (units generally in MHz). We can approximate the Fourier transform of  $|J(t)|$  with a rectangle that extends from  $f = -W/2$  and  $f = +W/2$ , as shown in Figure 10.

If the Chirp jammer has a bandwidth of  $W = 2$  MHz, i.e.,

$$P_j(f) = \begin{cases} J_0 & \text{if } |f| \leq \frac{1}{2} W_s \\ 0 & \text{if } |f| > \frac{1}{2} W_s. \end{cases} \quad (22)$$

Then the jammer power after block averaging preprocessing becomes,

$$\begin{aligned} \mathcal{E}_j^2 &= \int_{-\infty}^{+\infty} |H_L(f)|^2 P_j(f) df \\ &= J_0 \int_{-W_s/2}^{+W_s/2} |G_L(f)|^2 df \\ &= \frac{J_0}{L^2} \int_{-1}^{+1} \left| \frac{\sin(\pi f L)}{\sin(\pi f)} \right|^2 df = \frac{J_0}{L}. \end{aligned} \quad (23)$$

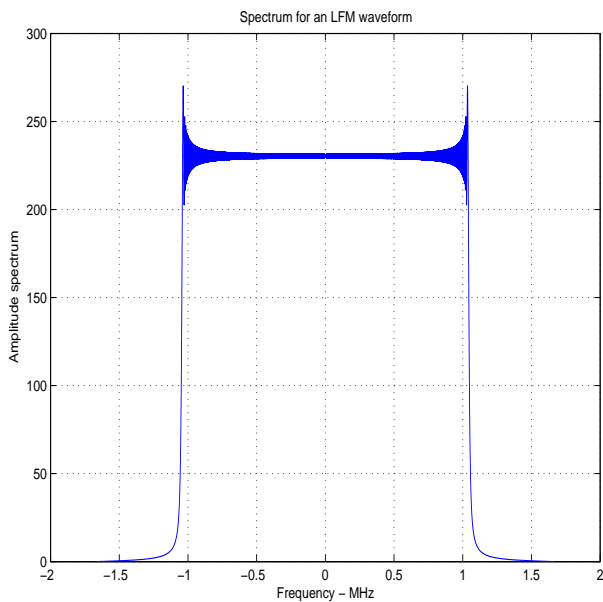


Fig. 10. Typical spectrum of a Chirp jammer with sweep duration of  $T = 10$  Microsecond, and swept bandwidth of  $W_j = W_s = 2$  MHz.

To prove equation (23), it is sufficient to know that the above integral is equal to  $L$ . Thus, block preprocessing reduces a broadband jammer by a factor of  $L$ , equal to the number of signal blocks.

## VII. CONCLUSION

A new block averaging pre-processing (BAP) to enhance the GPS signal power relative to the noise and interferers is introduced. The proposed block average model relies on the repetitive structure of the C/A code. The BAP technique is based on the accumulation of synchronized and phase-corrected signal blocks. We analyzed the advantage of using BAP in mitigating Gaussian noise, narrowband CW interference, partial-band jammer, and in-band Chirp jammer. Based on the BAP operation, we introduced two efficient FFT-based signal acquisition algorithms. The first algorithm is suitable for weak signals, whereas the second algorithm has fast implementation but operates on the square value of the averaged data, and therefore, is more sensitive to noise. The simulation results presented in this paper show that the proposed GPS synchronization approach provides good robustness against both interference and noise which is highly attractive when operating in hostile and urban environments.

## REFERENCES

- [1] Dennis M. Akos, "A Software Radio Approach to Global Navigation Satellite System Receiver Design," *PhD Dissertation*, Ohio University, August 1997. <http://gps.aau.dk/softgps/>
- [2] D. M. Akos et al., "Low Power GNSS Signal Detection and Processing," in *Proceedings of the ION conference GPS'2000*, Sept. 2000.
- [3] Moeness G. Amin, Liang Zhao and A. R. Lindsey, "Subspace array processing for the suppression of FM jamming in GPS receivers," in *IEEE Transactions on Aerospace and Electronic Systems*, 40(1), pp: 80 - 92, Jan. 2004.
- [4] Moeness G. Amin and W. Sun, "A Novel Interference Suppression Scheme for Global Navigation Satellite Systems Using Antenna Array," in *IEEE Journal on Selected Areas in Communications*, Vol. 23 No. 5, 2005.
- [5] K. Borre, D. M. Akos, N. Bertelsen, P. Render and S. H. Jensen, *A software-defined GPS and Galileo receiver, a signal-frequency approach*, Birkhäuser, 2007.
- [6] M. S. Braasch and A. J. Van Dierendonck, "GPS receiver architectures and measurements," in *Proceedings of IEEE*, 87(1), pp: 48-64, Jan. 1999.
- [7] Rod Bryant, "Assisted GPS (Using Cellular Telephone Networks for GPS Anywhere)," in *GPS WORLD*, May 1, 2005.
- [8] I. H. Choi et al., "A Novel Weak Signal Acquisition Scheme for Assisted GPS," in *Proc. of ION GPS'02*, Sept. 2002.
- [9] G. Dedes and A. G. Dempster, "Indoor GPS Positioning: Challenges and Opportunities," in *Proc. of the IEEE VTC'05 Conf.*, USA, 2005.
- [10] A. El-Rabbany, *Introduction to GPS : the Global Positioning System*, Boston, MA : Artech House, 2002.
- [11] G. Feng and F. Van Graas, "GPS Receiver Block Processing," in *proceedings of the ION conference GPS'99*, Nashville, TN USA, Septemebr 1999.
- [12] P. D. Groves, "GPS Signal to Noise Measurement in Weak Signal and High Interference Environments," in *Proceedings of the ION conference GNSS2005*, Long Beach, CA USA, 2005.
- [13] S. Gunawardena, F. Van Gaas and A. Soloviev, "Real Time Block Processing Engine for Software GNSS Receivers," in *Proceedings of the ION conference NTM 2004*, San Diego USA, January 2004.
- [14] R. Iltis and L. Milstein, "Performance analysis of narrowband interference rejection techniques in DS spread-spectrum systems," *IEEE Transactions on Communications*, vol. 32, no. 11, pp. 1169-1177, November 1984.
- [15] E. D. Kaplan (Ed.), *Understanding GPS: Principles and Applications*, Artech House Publisher, Second Edition 2006.
- [16] Steven Kay, *Intuitive Probability and Random Processes Using MATLAB*, Springer, 2006.
- [17] M. Kokkonen, S. Pietila, "A New Bit Synchronization Method for a GPS Receiver," in *Proceedings of the IEEE conference PLANS'2002*, April 2002.
- [18] R. Jr. Landry, P. Boutin and A. Constantinescu, "New anti-jamming technique for GPS and Galileo receivers using adaptive FADP filter," in *Elsevier Journal of Digital Signal Processing*, Vol. 16, Issue 3, Pages 255-274, May 2006.
- [19] A. V. Oppenheim, A. S. Willsky With S. H. Nawab, *Signals and Systems*, 2nd Edition, NJ: Prentice-Hall, 1997.
- [20] B. W. Parkinson and J. J. Spilker (Eds.), *Global Positioning System: Theory and Applications*, Vol. 1 and Vol. 2, Progress in Astronautics and Aeronautics, 1996.
- [21] Mark L. Psiaki, "Block Acquisition of Weak GPS Signals in a Software Receiver," in *Proceeding of the ION Conference GPS 2001*, Salt Lake City, UT USA, September 2001.
- [22] Mohamed Sahmoudi, *Robust Separation and Estimation of non-Gaussian and/or non-Stationary Sources*, Ph.D. dissertation, Univ. Paris-Sud (Paris XI), Orsay, France, December 2004.
- [23] M. Sahnoudi and Moeness G. Amin, "Improved Maximum Likelihood Time Delay Estimation for GPS Positioning in Multipath, Interference and Low SNR Environments," in *Proceeding of the ION/IEEE Conference PLANS'2006*, San Diego, April 2006.
- [24] M. Sahnoudi and Moeness G. Amin, "A Novel Maximum-Likelihood Synchronization Scheme for GPS Positioning in Multipath, Interference and Weak Signal Environments," in *Proceedings of the IEEE conference VTC'2006 Fall*, Montréal, Canada, September 2006.
- [25] S. Soliman et al., "gpsOne<sup>TM</sup>: a hybrid position location system", in *Proc. of IEEE Sixth ISSSTA*, Vol. 1, Sept. 2000.
- [26] W. Sun and Moeness G. Amin, "A Self-Coherence Anti-Jamming GPS Receiver," *IEEE Trans. on Signal Processing*, Vol. 53, No. 10, October 2005.
- [27] J. Bao-Yen Tsui, *Fundamentals of GPS Receivers: A software approach*, Second Edition, Wiley, 2002.
- [28] P. W. Ward, "GPS receiver interference monitoring, mitigation and analysis techniques," *Journal of the ION*, Vol. 41, No. 4, Winter 1995.
- [29] Chun Yang and Shaowei Han, "Block-Accumulating Coherent Integration over Extended Interval (BAPCIX) for Weak GPS Signal Acquisition," *Proceedings of the ION conference GNSS'2006*, Fort Worth TX, USA, September 2006.
- [30] Nesreen I. Ziedan, *GNSS Receivers for Weak Signals*, Artech House, August 2006.